The Effect of Heat Treatment on Physical, Chemical and Structural Properties of Calcium Sulfate Based Scaffolds

Hakan OFLAZ[1,2,*], Betül ALDEMİR DİKİCİ[1,2], Serkan DİKİCİ[1,2]

[1] İzmir Kâtip Çelebi Üniversitesi, Mühendislik ve Mimarlık Fakültesi, Biyomedikal Mühendisliği Bölümü, 35620, İzmir
[2] İzmir Kâtip Çelebi Üniversitesi, Fen Bilimleri Enstitüsü, Biyomedikal Teknolojileri Anabilim Dalı, 35620, İzmir

Abstract: 3D printed calcium sulfate (CS) is a promising material for on custom bone substitutes. Since it dissolves easily in body fluids, manufactured samples require to being improved to reduce solubility. The main aim of this study was reducing the dissolubility of CS based samples by using sintering and investigating the effect of heat treatment on their physical, chemical and structural properties. To observe the effect of heat treatment on samples, contact angles were measured, X-Ray diffraction analysis (XRD) was performed, and scanning electron microscope (SEM) micrographs were captured before and after the sintering process, and the results were compared. Furthermore, sintered and non-sintered samples were soaked in phosphate buffered saline (PBS) to observe the impact of sintering on the solubility of the material. Also, three different pore sized scaffolds were manufactured to test the limits of the 3D printer for manufacturing of scaffolds with open pores. Sintering process results in a volume reduction and according to SEM results, CS grains were fused together after heat treatment. Although non-sintered CS sample starts to dissolve in high rate and nearly 1/3 of the sample was at the bottom of the glass in a matter of minutes, sintering creates more rigid structure and there were not visible dissolution in PBS at the end of a week. The contact angle of samples cannot be measured, so it can be concluded that 3D printed material showed a super-hydrophilic property. XRD diagram suggested that there is not any new phase created in the printing and sintering processes except related hydrates of CS. As a result of the 3D printing, 500 µm, 750 µm and 1000 µm pore sized scaffolds were manufactured, successfully. However, it was seen that 500 µm pores could not be open by using depowdering after the printing process.

Isıl Muamelenin Kalsiyum Sülfat Bazlı İskelelerin Fiziksel, Kimyasal ve Yapısal Özellikleri Üzerine Etkisi

Özet: 3 boyutlu yazdırılmış kalsiyum sülfat (KS), kişiye özel kemik uygulamaları için umut verici bir malzemedir. Bununla birlikte bu malzemenin suya olan düşük dayanıklılığı nedeni ile vücut sıvıları içerisinde kolayca çözünebilmektedir ve bu çözünürlüğün azaltılması için malzemenin geliştirilmesine ihtiyaç duyulmaktadır. Bu çalışmanın asıl amacı, sinterleme işlemi ile KS bazlı örneklerin çözünürlüğünü azaltmak ve bu ısıl işlemin malzemenin fiziksel, kimyasal ve yapısal özellikleri üzerine olan etkisini araştırmaktır. Isıl muamelenin örnekler üzerine olan etkisini incelemek amacı ile sinterleme işlemi öncesi ve sonrası örneklere temas açısı, X ışınları kırınımı (XRD) analizleri uygulanmış, örnek yüzeylerinin taramalı elektron mikroskobu (SEM) görüntüleri alınmış ve sonuçlar karşılaştırılmıştır. Ayrıca, sinterleme işleminin malzeme çözünürlüğü üzerine olan etkisini incelemek amacı ile sinterlenmiş ve sinterlenmemiş örneklerin fosfat tamponlu tuz (PBS) içerisindeki çözünürlükleri gözlemlenmiştir. Ayrıca çalışma kapsamında 3 farklı gözenek çapında iskeleler üretilmiş ve 3 boyutlu yazıcının açık gözenekli iskele üretmedeki limitleri belirlenmiştir. Sinterleme işlemi örneklerin hacmen azalmasına neden olurken, SEM görüntülerine göre KS parçacıkları ısıl işlem sonrasında kaynaşmışlardır. PBS içerisinde sinterlenmemiş KS örneklerinin yaklaşık üçte biri dakikalar içerisinde çözünerek dibe çökerken, sinterleme işlemi örnekleri daha kararlı hale getirmiş ve bir hafta PBS içerisinde bekleyen örneklerde gözle görülür bir çözünmeye rastlanmamıştır. Temas açısı ölçüm sonuçları malzemenin ısıl işlem öncesi ve sonrası süper hidrofilik karakterde olduğunu göstermektedir. XRD diyagramı, 3B yazdırma ve sinterleme işlemleri sonucu KS'nin sulu bileşikleri dışında yeni bir faza rastlanmadığını göstermiştir. 500 µm, 750 µm ve 1000 µm gözenekli iskeleler 3B olarak başarılı bir şekilde yazdırılmıştır. Fakat 500 µm gözenekli iskele yazdırma işlemi sonrası bağlanmamış tozların uzaklaştırılması basamağında başarılı bir sonuç vermemiş ve açık gözenekler elde edilememiştir.

Corresponding author: hakan.oflaz@ikc.edu.tr

1. Introduction

Many different bone diseases such as bone infections, fractures and osteoporosis are more frequently seen due to the rise in the average age of population or traumatic reasons [1, 2]. Since bone cannot manage to heal itself when a defect exceeds critical size, autographs or allographs are used for bone reconstruction in order to improve bone healing [3, 4]. Although four million bone grafting are performed in the world annually, autographs and allographs have significant limitations and risks such as donor site morbidity, high infection risk and immune response [3, 5]. At this point, tissue engineering offers various strategies with biocompatible and well-designed 3D bone scaffolds to lead tissue formation [6].

Since calcium sulfate (CS) is a biocompatible and resorbable ceramic, this biomaterial has been used in bone regeneration more than 100 years [7-9]. Moreover, it releases calcium ions which may provide an advantage for osteoblast formation [8]. Calcium sulphate hemihydrate (CSHH) was studied by Sidqui et al [10]. It was reported that osteoblastic cells attach on CSHH and osteoclasts resorb the material. Wu H. D. and his colleagues demonstrated that combination of amorphous calcium phosphate and CS improves osteoconductivity of materials and degradation period of this composite matching with natural bone regeneration rate [7].

Although this inexpensive medical grade resorbable CS has a long history in orthopedics, powder based 3 dimensional printing (3DP) technique may bring innovation to its usage in tissue engineering [11]. In this technique, one thin layer of powder material is dispersed on a platform, following that the binder is sprayed onto the laid powder layer. The binder binds the powders to form a single 2D layer, therefore a sliced 2D profile of a computer model is created. This process occurs many times to fabricate a 3D structure layer by layer until the whole model is completed [4]. 3DP can produce models that are difficult to create by conventional industrial methods [12]. Due to its high controllability, design independency, fast reducibility, reproducibility 3D printed CS products may be used in customized artificial bone grafts.

Recently, the 3DP technique attracts the field of tissue engineering to apply the 3DP technology in designing precise custom made scaffolds with ceramic materials [13]. The main aim in personalized bone substitutes is to produce defect-matching scaffolds. There are certain essential steps for production of patient-specific implants or grafts. Firstly, 3D model of defect side should be captured by computerized tomography (CT) scan and imported to the program. If the defect side has a healthy mirror image on body (such as deficient right hand, health left hand), CT data of the health area is captured to be used as a scaffold model. Otherwise, this model should be created by CAD (Computer Aided Design) software such as Solidworks or Inventor. After designing the inner architecture (flat or porous) and outer shape of the scaffold or implant, model is produced slice by slice by convenient additive manufacturing (AM) technique according to material type.

Although 3D printed CS grafts are good candidates for tailor made scaffolds, in contrast to its various advantages, one of the major challenge in usage of CSHH as a scaffold material is its high solubility as such in other ceramics [14]. This problem could be overcome by using sintering as a post-process [15-18].

The main aim of this study was reducing the dissolubility of CS based samples by using sintering and investigating the effect of sintering on solubility of the materials and analyzing the material phases after printing and sintering processes to compare with the initial phase of the powder. To investigate the effect of sintering on samples, contact angles were measured, X-Ray diffraction analyses was performed, and SEM micrographs were captured before and after the sintering process. Furthermore, sintered and non-sintered samples were soaked in PBS to observe impact of sintering on the solubility of the material. Also, three different pore sized scaffolds were manufactured to test the limits of the 3D printer for manufacturing of scaffolds with open pores.

2. Material and Method

2.1. Manufacturing and sintering

Commercial powder (calcium sulfate hemihydrate, CSHH) (3DS, Visijet, PXL, Core, Osha, USA) which has a particle size distribution 10%, 50% and 90% of powder below 0.64, 27.36 and 68.83 μm, respectively [19] was purchased from 3D Systems. CAD files of the test samples were created by CAD software (Autodesk Inventor Professional 2014, USA) as a requirement of 3DP process. Cylindrical scaffolds Ø 10 mm, 5 mm height was designed to test solubility. 500 μm, 750 μm and 1000 μm porous scaffolds were created in two different pore intensities to find the optimum design for solubility (Figure 1).
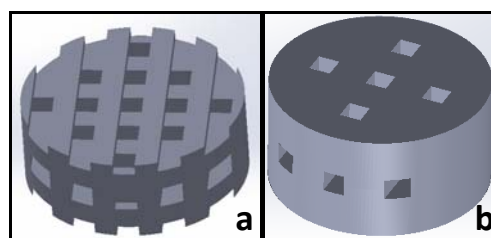

Figure 1. CAD models of 3D printed porous scaffolds a. higher porosity, b. lower porosity

Following the design process, they were exported as .stl (surface tessellation language, stereolithography) which is the file format allowing to define 3D models using just triangle meshes. Data were imported into 3D printing software (3DP Projet X60, Ver. 1.01, USA) where models were sliced by a slicing algorithms.

After loading CSHH powder to 3D printer, 2D sliced layers were printed layer by layer (Projet 160, 3D Systems, USA). Printing process continued till the 3D model was physically formed. CSHH and water based binder (3DS, Visijet, PXL, Clear, Osha, USA) were used as consumables in 3DP process. The binder of 3D printer was Visijet PXL which is formulated as 2-pyrrolidone. It is colourless aqueous solution which has 98% water content. The pH of the binder at 20 °C is 9.8, its boiling point is 100 °C and it has a density of 1 g/cm^3 according to safety data sheet of the material. The viscosity is similar to water [19].

One layer of powder thickness was 100 μm in all prints, so the resolution of printing process was also 100 μm. At the end of the printing process all scaffolds were kept in the building platform for 90 min at ambient temperature. Samples were cleaned by blowing air to get rid of loose powders after printing as a post process.

Since ceramic materials have high solubility especially in biological fluids, after printing and blowing air processes, scaffolds were sintered for 2 hours at 1150 °C at furnace (Protherm Furnaces, Turkey) to reduce dissolution ratio. Since the CSHH release corrosive gas of ammonium sulphur during heating process, materials were pre-baked for 2 hours at 300 °C at oven (Luxell Lx 3685, Turkey) not to corrode resistances of furnace. Required temperature in order to remove the water and the ammonium sulfate was determined by Teoreanu et al.[20]. After that samples were ready to be fused by sintering.
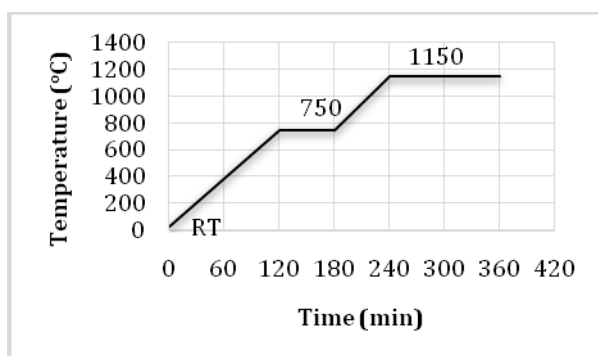

Figure 2. Sintering cycle of CSHH scaffolds

Tamman temperature is the temperature which two particles start to fuse each other for sintering. So, sintering temperature should be between tamman temperature and melting temperature ($T_{melting} > T_{sintering} > T_{tamman}$) [21]. Since the tamman and

the melting temperatures of CSHH was indicated as 416 °C and 1450 °C respectively, the final sintering temperature should be determined between these values [22]. β-CSHH have a possibility of transforming into α-CSHH above 1200 °C [21]. Therefore, 1150 °C was applied for best densification and to have best physical properties (Figure 2).

2.2. Analysis

2.2.1. Wettability measurements

The wettability of green and sintered CSHH samples (n=3) were measured using a contact angle meter (Biolin Scientific, Thetalite, Sweden). 4.5 μl of distilled water applied on CSHH sample's surface to measure the water contact angle under a CCD camera at ambient temperature (Figure 3).

2.2.2. Scanning electron microscopy (SEM) analyses

To observe the difference between the surface microstructures of the sintered and non-sintered scaffolds, scanning electron microscopy (SEM, JSM-6060 JEOL) were used. Samples were sputter-coated with gold–palladium prior to imaging.

2.2.3. X-ray diffraction (XRD) analysis

XRD was done to observe if there were different phases of CSHH after printing and sintering processes. Three different sample were examined with XRD; non-printed CSHH, printed and non-sintered CSHH, printed and sintered CSHH. Non-printed powders were used directly. Since powder form sample is required for XRD analysis, 3D printed green and sintered samples were pestle to have fine particles. XRD patterns of samples were obtained by using Philips X-Pert Pro Diffractometer using Ni-filtered Cu Kα radiation (λ= 1.54 Å) operated at 45 kV and 40 mA. The data were collected in 2θ angle ranged from 5° to 80°. The scan step size and time per step were set to 0.03° and 10 s, respectively.

2.2.4. Solubility tests

To investigate the effect of sintering on the solubility of the 3D printed samples, non-porous block samples were soaked in PBS at 37 °C and observed for 1 week.

3. Results

3.1. Manufacturing and sintering

As a result of the 3D printing, although 500 μm, 750 μm and 1000 μm pore sized scaffolds were manufactured successfully, it was seen that 500 μm pores could not be open by using depowdering after the printing process.
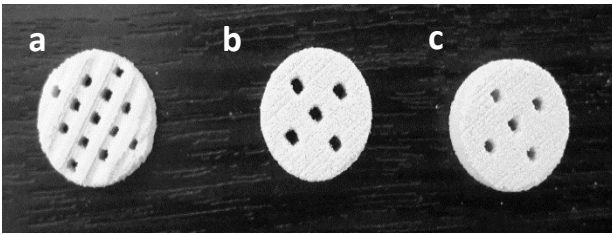
Figure 3. Interconnected porous scaffold design a. High numbers of 750 μm pores (relatively), b. The lower number of 1000 μm pores (relatively), c. The lower number of 750 μm pores (relatively)

Following the sintering process, the specimens were shrunk and while the initial radius was 10 mm (Figure 4a), it reduced to 8.5 mm (Figure 4b) at the end of the heat treatment.
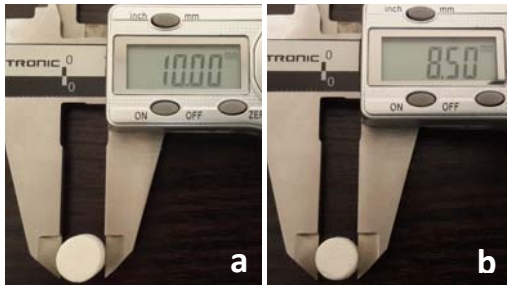

Figure 4. Comparison of measures of a. non-sintered and b. sintered samples

3.2. Analysis

3.2.1. Wettability measurements

To observe the hydrophilic character of 3D printed samples wettability measurements were performed. Complete resorption of dropped liquid is an indicator of hydrophilicity.
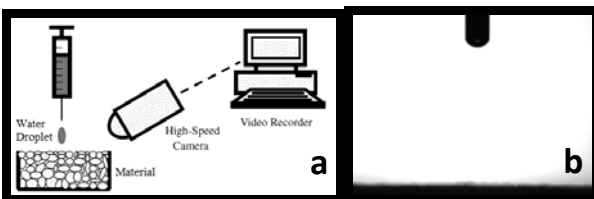

Figure 5. Contact angle a. setup [23], b. view of 3D printed sample.

As a result of the measurement, the contact angle of the samples cannot be measured, so it can be concluded that 3D printed material showed a super-hydrophilic property. In the other words, dropped pure water was completely absorbed by the surface of the material.

3.2.2. SEM analyses

The surface microstructures of the non-sintered and sintered scaffolds were captured by using SEM. According to micrographs, while in the Figure 6a particles are piece by piece, they appear like an integrated unit after sintering processes (Figure 6b).
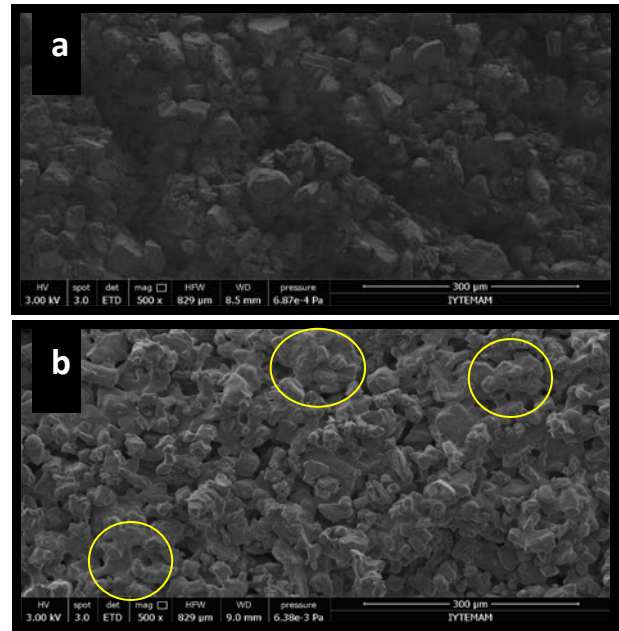

Figure 6. SEM micrographs illustrating surface microstructure of 3D printed a. Green, b. Sintered samples (circles indicated the fused particles).
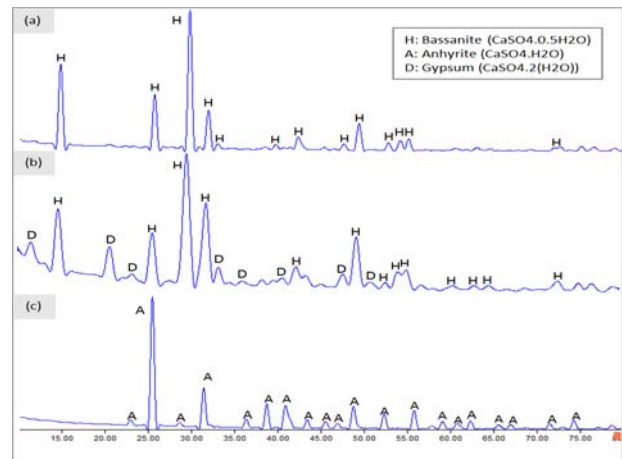

Figure 7. XRD patterns of a. the starting powder, b. as-printed sample, c. sintered sample
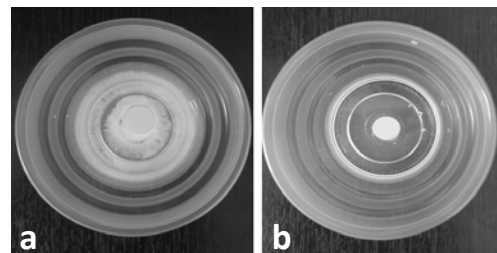

Figure 8. Comparison of dissolution, a. non-sintered 3D printed sample in PBS, b. sintered 3D printed sample in PBS.

3.2.3. X-ray diffraction (XRD) analysis

XRD analysis of the commercial powder material was performed to compare the initial phase of the material with printed and sintered phases. XRD specific patterns demonstrated that before sample fabrication commercial powder consisted of calcium hemihydrate ($CaSO_4 . 0.5H_2O$) (**Hata! Başvuru kaynağı bulunamadı.**6a). Following the raw powder,

material phases was observed after fabrication. Since the binder of the 3D printer (2-pyrollidone) has 98% water content, the reverse reaction occurred and initial powder CSHH transformed into gypsum after printing process (**Hata! Başvuru kaynağı bulunamadı.**6b). Finally, 3D printed and sintered powder was examined with XRD spectroscopy. Specific peaks of the material matched with anhydrite ($CaSO_4$) after sintering process (**Hata! Başvuru kaynağı bulunamadı.** 6c).

3.2.4. Solubility tests

It was clearly seen that when the non-sintered sample were immersed in PBS, it started to dissolve in high rate and nearly 1/3 of the sample was at the bottom of the glass in a matter of minutes (Figure 8a). However, when the sintered sample was soaked in PBS for 1 week, they highly stand up to dissolution and there was no visible dissolution (Figure 8b).

4. Discussion and Conclusion

3D printed CS is a promising material for on custom bone substitutes. However, due to its lower affinity for water and they dissolve easily in body fluids and manufactured samples require to be improved to reduce solubility. Sintering reduced dissolubility in addition to the results in a reduction in porosity and increase in mechanical strength of parts.
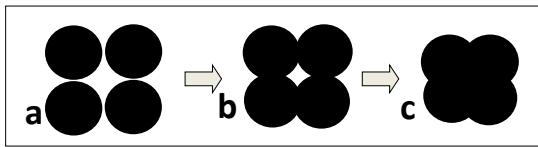

Figure 9. Grain shape changes during sintering process

This process results in a volume reduction; this is called sintering shrinkage. As it can be clearly seen from Figure 6a to Figure 6c, grains are fused together by the reduction in porosity. For the same reason, in this study 3D printed CS scaffolds were sintered at 1250° and fused CS particles were clearly seen in the SEM micrograph (Figure 6b). Although non-sintered CS sample starts to dissolve in high rate and nearly 1/3 of the sample was at the bottom of the glass in a matter of minutes, 15% shrinkage of sample creates more rigid structure and there were not visible dissolution in PBS at the end of a week.

Biocompatibility of materials is mostly about the cell behaviour when contact with the material and surface characteristics have an important role in cell adhesion. Cell attachment and spreading is the first step of cell-material interaction and its success will highly effect on cell proliferation [24]. Cells can attach and grow more easily on hydrophilic surfaces in comparison with hydrophobic surfaces [25]. Thus, according to contact angle results, it can be concluded that our material has convenient surface property before and after sintering in terms of hydrophilicity.

CS has three phases with various hydration levels; $CaSO_4 \cdot 2H_2O$ (gypsum/CSHH), $CaSO_4 \cdot 0.5H_2O$ (basanite) and $CaSO_4$ (anhydrite) [10]. Figure 7 shows the XRD patters of the starting powder, as-printed sample and sintered sample to compare the initial phase of the material with printed and sintered phases. The XRD spectrum demonstrates that the sample before fabrication was consisted of CSHH which is an inorganic compound for also known as plaster of Paris and basanite, dehydrated phase of $CaSO_4$. Since the binder of the 3D printer (2-pyrollidone) have 98% water content, initial powder CSHH react with binder and transformed into gypsum after printing process.

$$CaSO_4 \cdot \tfrac{1}{2}H_2O + \tfrac{9}{2}H_2O \longrightarrow CaSO_4 \cdot 2H_2O \qquad (1)$$
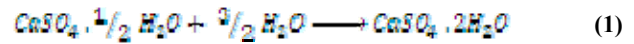
However, according to the specific XRD patterns, the powder consisted of a mixture of both gypsum and basanite phases due to nonhomogeneous contact between binder and powder during the 3DP process (Figure 6b) [10].

Thirdly, 3D printed and sintered powder was examined with XRD spectroscopy. Specific peaks of the material were matched with anhydrite after sintering process (Figure 6c). Since gypsum transforms into anhydrite form above 200 °C, sintered samples were in anhydrite phase.
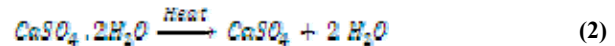
$$CaSO_4 \cdot 2H_2O \xrightarrow{\text{Heat}} CaSO_4 + 2H_2O \qquad (2)$$

XRD diagram suggested that there is not any new phase created in the printing and sintering processes except related hydrates of CS.

Also, three different pore sized scaffolds were manufactured to test the limits of the 3D printer for manufacturing of scaffolds with open pores. Although 3D printer has high resolution, removing loose powder is critical step. As a result of the 3D printing, 500 μm, 750 μm and 1000 μm pore sized scaffolds were manufactured successfully. However, it was seen that 500 μm pores could not be open by using depowdering after printing process. Thus, 750 μm and 1000 μm pore sized scaffolds were more producible as against 500 μm.

Effect of heat treatment on physical, chemical and structural properties of calcium sulfate based scaffolds was investigated in this study. We consider that the findings of this study call for further studies to use improved CS as a bone graft material.

Acknowledgment

– www.hgomedikal.com.tr) for their consultancy in engineering and manufacturing approaches.

References

[1] Bose, S., Roy, M., Bandyopadhyay, A. Recent advances in bone tissue engineering scaffolds. Trends in biotechnology, 30(2012), 546-54.

[2] Rauh, J., Milan, F., Gunther, K.P., Stiehler, M. Bioreactor systems for bone tissue engineering. Tissue engineering. Part B, Reviews, 17(2011), 263-80.

[3] Brydone, A.S., Meek, D., Maclaine, S. Bone grafting, orthopaedic biomaterials, and the clinical need for bone engineering. Proceedings of the Institution of Mechanical Engineers. Part H, Journal of engineering in medicine, 224(2010), 1329-43.

[4] Lichte, P., Pape, H.C., Pufe, T., Kobbe, P., Fischer, H. Scaffolds for bone healing: concepts, materials and evidence. Injury, 42(2011), 569-73.

[5] Inzana, J.A., Olvera, D., Fuller, S.M., Kelly, J.P., Graeve, O.A., Schwarz, E.M., et al. 3D printing of composite calcium phosphate and collagen scaffolds for bone regeneration. Biomaterials, 35(2014), 4026-34.

[6] Subia, B.K., J.; Kundu, S. C. . Biomaterial Scaffold Fabrication Techniques for Potential Tissue Engineering Applications. In: Tissue Eng, Eberli, D. Ed., 2010.

[7] Wu, H.D., Lee, S.Y., Poma, M., Wu, J.Y., Wang, D.C., Yang, J.C. A Novel Resorbable α-Calcium Sulfate Hemihydrate/Amorphous Calcium Phosphate Bone Substitute for Dental Implantation Surgery. Materials Science and Engineering C, 32(2012).

[8] Thomas, M.V., Puleo, D.A., Al-Sabbagh, M. Calcium sulfate: a review. Journal of long-term effects of medical implants, 15(2005), 599-607.

[9] Pietrzak, W.S., Ronk, R. Calcium sulfate bone void filler: a review and a look ahead. The Journal of craniofacial surgery, 11(2000), 327-33; discussion 34.

[10] Sidqui, M., Collin, P., Vitte, C., Forest, N. Osteoblast adherence and resorption activity of isolated osteoclasts on calcium sulphate hemihydrate. Biomaterials, 16(1995), 1327-32.

[11] al Ruhaimi, K.A. Effect of calcium sulphate on the rate of osteogenesis in distracted bone. International journal of oral and maxillofacial surgery, 30(2001), 228-33.

[12] Utela, B., Storti, D., Anderson, R., Ganter, M. A Review of Process Development Steps for New Material Systems in Three Dimentional Printing (3DP). Journal of Manufacturing Processes, 10(2008).

[13] Chen, Z.G., Liu, H.Y., Liu, X., Lian, X.J., Guo, Z.W., Jiang, H.J., et al. Improved workability of injectable calcium sulfate bone cement by regulation of self-setting properties. Mat Sci Eng C-Mater, 33(2013), 1048-53.

[14] Bose, S., Vahabzadeh, S., Bandyopadhyay, A. Bone tissue engineering using 3D printing. Mater Today, 16(2013), 496-504.

[15] Suwanprateeb, J., Sanngam, R., Suvannapruk, W., Panyathanmaporn, T. Mechanical and in vitro performance of apatite-wollastonite glass ceramic reinforced hydroxyapatite composite fabricated by 3D-printing. Journal of materials science. Materials in medicine, 20(2009), 1281-9.

[16] Khalyfa, A., Vogt, S., Weisser, J., Grimm, G., Rechtenbach, A., Meyer, W., et al. Development of a new calcium phosphate powder-binder system for the 3D printing of patient specific implants. Journal of materials science. Materials in medicine, 18(2007), 909-16.

[17] Asadi-Eydivand, M., Solati-Hashjin, M., Shafiei, S.S., Mohammadi, S., Hafezi, M., Abu Osman, N.A. Structure, Properties, and In Vitro Behavior of Heat-Treated Calcium Sulfate Scaffolds Fabricated by 3D Printing. PloS one, 11(2016), e0151216.

[18] Aldemir, B. Development, Production and Characterization of Ceramic Based 3D Tissue Scaffolds. Izmır, Izmir Katip Celebi University; 2016.

[19] Asadi-Eydivand, M., Solati-Hashjin, M., Farzad, A., Abu Osman, N.A. Effect of technical parameters on porous structure and strength of 3D printed calcium sulfate prototypes. Robot Cim-Int Manuf, 37(2016), 57-67.

[20] Teoreanu, I., Preda, M., Melinescu, A. Synthesis and characterization of hydroxyapatite by microwave heating using CaSO4.2H2O and Ca(OH)2 as calcium source. Journal of materials science. Materials in medicine, 19(2008), 517-23.

[21] Iribarne, A.P.I.J.V.A.A.J. Reactivity of calcium sulfatefrom FBC systems Fuel, 76(1997).

[22] Marsh, D.V.U., D. L. Rate And Diffusional Study Of The Reaction Of Calcium Oxide With Sulfur Dioxide. Chemical EngineeringScience, 40(1985).

[23] Zhou, Z., Buchanan, F., Mitchell, C., Dunne, N. Printability of calcium phosphate: calcium sulfate powders for the application of tissue engineered bone scaffolds using the 3D printing technique. Materials science & engineering. C, Materials for biological applications, 38(2014), 1-10.

[24] Anselme, K. Osteoblast adhesion on biomaterials. Biomaterials, 21(2000), 667-81.

[25] Yamada, N., Okano, T., Sakai, H., Karikusa, F., Sawasaki, Y., Sakurai, Y. Thermoresponsive Polymeric Surfaces - Control of Attachment and Detachment of Cultured-Cells. Makromol Chem-Rapid, 11(1990), 571-6.